

FEASABILITY STUDY OF EFFECTIVENESS OF PENDULUM VIBRATION ABSORBER ADAPTED TO 90-DEGREE V-TWIN AERO ENGINE

SPONSORED BY
SPIRIT ENGINEERING

UNIVERSITY OF COLORADO BOULDER, MAY 4, 2018

Ross M Fischer
CU Boulder
Grand Junction, CO, USA

Eric J Jacobs
CU Boulder
Grand Junction, CO, USA

Tyler T Raymond
CU Boulder
Grand Junction, CO, USA



Mechanical Engineering
University of Colorado Boulder

TABLE OF CONTENTS

INTRODUCTION	3
1.1 – Problem scope	3
1.2 – Field Background	3
1.3 – History of Existing Devices for Controlling Vibration	4
1.4 – Rotating Pendulum Vibration Absorber	4
1.5 – Project Goals	7
1.6 – Validation	7
METHODS	8
2.1 - Gather RPVA background information	8
2.2 - Review work done by the client	8
2.3 - Establish pendulum criteria	9
2.4 - Select pendulum design based on criteria	9
2.5 - Create a dynamic model of the system	10
2.6 - Use Wilson's equations to estimate dynamic model performance	10
2.7 - Define Pendulum Design	11
2.8 - Assess results against project criteria	11
RESULTS	12
3.2 - Review work done by the client	12
3.3 - Establish pendulum criteria	13
3.4 - Select pendulum design based on criteria	13
3.5 - Create a dynamic model of the system	14
3.6 - Use Wilson's equations to estimate dynamic model performance	15
3.7 - Define Pendulum Design	17
3.8 - Assess results against project criteria	17
CONCLUSION	18
BIBLIOGRAPHY	19
APPENDICES	20

INTRODUCTION

1.1 – Problem scope

Spirit Engineering is a small engineering firm located in Grand Junction, Colorado. In 2009, Spirit Engineering, the client, began design work on a prototype Light Sport Aircraft (LSA). LSA are planes regulated by the Federal Aviation Administration's LSA Rule. The LSA rule was introduced in 2004 [1] to promote the expansion of the general aviation sector in the United States by simplifying regulations and lowering the cost for development and testing. These savings are then passed onto the consumer. The client intends to manufacture a lightweight, inexpensive, single-seat, aircraft regulated by the LSA Rule. The client intends to fit a Kohler V-twin engine (or similar) to the aircraft for reasons of compact size, improved pilot visibility, lower part count, and a reduction in primary balance vibration issues.

The power of a V-twin engine is delivered in two pulses per combustion cycle. By comparison, an engine with a higher cylinder count may deliver the same power spread over more combustion pulses. This is disadvantageous for a V-twin engine since the delivered power is concentrated to fewer combustion events. The problem is exacerbated by the 90-degree configuration which produces uneven combustion events. In other words, the lapsed time between the first and second combustion is not the same as the lapsed time between the second and third combustion.

These large, sharp, unevenly distributed power pulses delivered by the V-twin engine propagate vibration into the engine powertrain, leading to high stresses in the crankshaft. In the past, pendulum absorbers have been fitted to aero-engine counterweights to reduce crankshaft stress, increase engine life, decrease airframe vibrations, and improve pilot comfort. In the fall of 2017 the client tasked the senior design team with determining the feasibility of adapting a pendulum absorber to a Kohler CH1000 engine (Figure 1).



FIGURE 1. KOHLER CH1000 V-TWIN ENGINE [2]

1.2 – Field Background

During normal engine operation, many forces contribute to vibrations within a crankshaft. These vibrations can be transmitted throughout the engine block, to the airframe, and into the pilot seat. The largest contributor to crankshaft vibrations is the force on the crankpin produced by combustion. This force creates a torque on the crankshaft causing it to rotate. As the torque is applied, the crankshaft acts as a torsional spring and allows angular twist to occur between the major inertias on the crankshaft.

The crankshaft may then be represented as a series of inertias connected by torsional springs. The number of inertias and springs and the magnitude of each inertia and spring constant will vary for different engine designs [3]. The major inertias and respective locations for a V-twin engine driving a propeller are the inertia of the propeller at its attachment point, an equivalent inertia (consisting of the crankpin and the two crank webs, pistons, and connecting rods) at the crankpin, and the inertia of the flywheel at its attachment point [4]. This system is presented in Figure 2. As angular twist occurs between the major inertias, a restoring torque is induced within the shaft causing the shaft to accelerate in the opposite direction. This torsional vibration occurs at the system's natural frequency. This response is predictable, and the natural frequency may be calculated from the magnitudes of the inertias and the spring constants of the shafts which connect adjacent inertias.

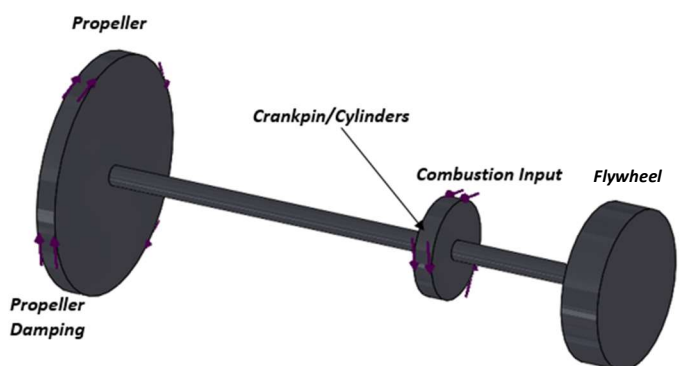


FIGURE 2. MODEL OF THE INERTIAL SYSTEM

Problems may arise when the frequency of the input torque matches that of the torque induced by twisting such that the resultant restoring torque, angular deflections, and stresses are amplified. This situation is complicated considering it may arise at various operating speeds. Specifically, orders of vibrations, (i.e. the number of events, or vibration cycles, per revolution of the crankshaft [5]) are created when the input torque frequency is a multiple of the natural frequency.

Considering vibratory responses are unique to the system properties, relatively simple solutions are often implemented by tuning the resonance away from the engine's operating range by adjusting the system's properties (i.e. inertia magnitudes or locations). In other cases, such as when engine characteristics may not be adjusted, special devices for controlling vibrations must be installed.

Until circa 1935, investigations into crankshaft vibration were led by the marine industry. Outcomes included investigations of shaft failures, development of torsionmeters, and papers describing torsional theory in multiple-mass systems. After 1935, the aeronautical industry began providing valuable contributions to the field of vibration study [5]. Notable contributions from this period were methods for deriving crankshaft stiffness, development of experimental procedures allowing data to be collected while the propeller is installed on the engine, and revisions of strain gauge designs allowing for reliable and accurate measurements of shaft stresses [5].

1.3 – History of Existing Devices for Controlling Vibration

In the early 1900's, the first organized studies of torsional vibrations in crankshafts were developed. These studies were chiefly a response to the problems afflicting engines with higher relative power and higher stresses within their crankshafts. Manufacturers recognized that generating reliable knowledge about engine vibration problems allowed for better engine design (i.e. higher engine power with reduced weight) [6].

Development history has established the importance of understanding vibratory phenomena as engines operate at higher speeds and with less weight. Only theoretical analysis is often needed during the engine design process to guide the system away from harmful resonant conditions. In other cases, such as when incorporating a pre-fabricated engine in a new vehicle design, a more involved approach is necessary where the solution may include development and installation of a device for controlling vibrations.

Many devices exist for controlling the problems vibrations create at various locations on the aircraft. For example, if vibrations were transmitted to the airframe then a solution may lie in isolating the engine from the airframe. However, if torsional vibrations are creating higher than acceptable stresses on the crankshaft, then it may be necessary to install a vibration absorber or damper to reduce the amplitude of the oscillations, thereby reducing the torsional stress. Both vibration absorbers and dampers operate on a similar principle; each device absorbs energy from the torsional vibrations, thereby reducing the amplitude of the vibration oscillation.

Vibration dampers are unique in that the absorbed energy is dissipated, usually by utilizing a viscous or elastic medium. Consequently, the act of dissipating this energy creates heat within the device that must be removed. Silicon based dampers were widely adopted within the automotive industry by the

second half of the 1940s [7]. These viscous dampers were found to be the most cost-effective solution to the prevailing vibration problems of the time. However, the aeronautical industry did not find dampers as favorable [5]. Since aircraft engines are often operated near a constant speed, a damper designed for that speed would operate continuously, thereby generating excessive amounts of heat and dissipating a considerable amount of the engine's power. In other words, dampers are suited for engines only intermittently operating over a wide range of speeds.

By contrast, vibration absorbers reduce vibrations by absorbing and then returning the vibrational energy during a different phase of the vibration cycle. Some absorber assemblies operate on the principle of torsionally flexible couplings, while many others utilize a mass acting as a pendulum oscillating on the crankshaft. The latter type of device is known as a rotating pendulum vibration absorber. These are of particular interest and have been widely employed within the aeronautical industry since the 1940's [5].

1.4 – Rotating Pendulum Vibration Absorber

The rotating pendulum vibration absorber (RPVA) may be viewed as a device in which a pendulum, such as the arm of a grandfather clock, is attached to a rotating carrier. The simplest theorization of an RPVA is shown in Figure 3. RPVA function

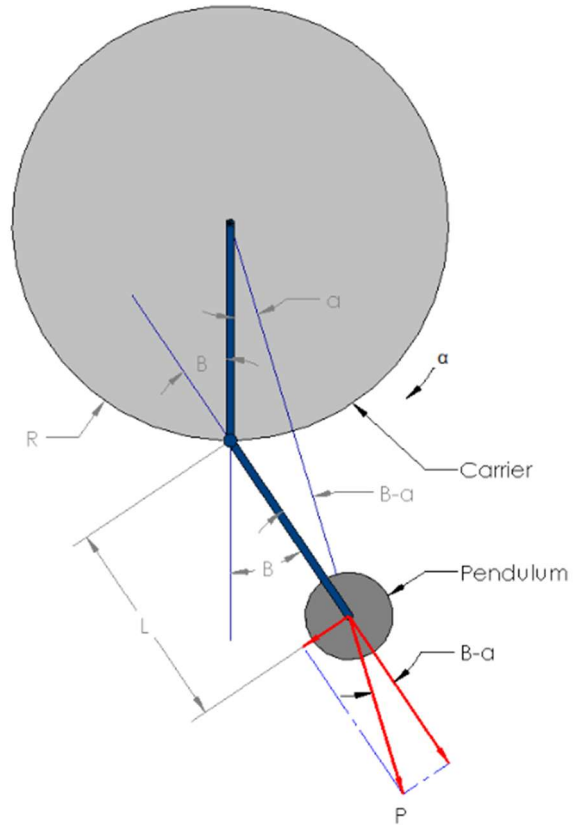


FIGURE 3. SIMPLE REPRESENTATION OF RPVA

is unique because they may be tuned to the order of a system as opposed to the frequency of a system. This is beneficial because they will function over the entire operating range of the engine. The restoring torque of an RPVA depends on centrifugal force and is also a function of the square of the speed of the carrier to which it is mounted. Therefore, as the input torque and speed of the crankshaft increases, the RPVA counters this torque proportionately. This is the great advantage of the RPVA. It has the potential to eliminate the vibrations of a given order entirely at all operating speeds [5]. Other forms of damper or absorber may only reduce vibratory amplitudes to equilibrium values and do so at a single operating speed. Other advantages of the RPVA include its efficiency of operation, long service life, and ability to counteract both torsional and bending oscillations [5].

The first mass produced engines with RPVAs appeared in World War II [5]. They were designed to suppress vibrations from large radial engines, such as the Wright Cyclone 9-cylinder radial of 1936. The 4.5th order of vibration in these engines was much larger in magnitude than others [6]. For this reason, the majority of the engine's vibration could be suppressed with a single RPVA. These engines also had a large counterweight. A portion of the counterweight mass was used as the RPVA, sparing the engine from the penalty of increased weight. The success of the RPVA aboard this engine established a trend during World War II and RPVAs became prevalent among aircraft during this time period [5].

There are disadvantages to the RPVA that, until recently, prevented their widespread use in the automotive industry. Research from the automotive industry showed RPVAs had greater potential to remove troublesome vibrations compared to other solutions circa 1940 [5]. However, unlike the radial engines in the aerospace industry, the inline engines of the automotive industry required the suppression of multiple orders of vibration. The RPVA suppresses vibrations of the order to which it is tuned and has little impact on vibrations outside of this order. Suppression of multiple orders requires multiple RPVAs and the subsequent cost was too great for the industry to bear [5]. Around this time, a viscous friction damper was developed that used silicone fluid as the damping medium. This design increased performance and reduced the cost of current dry-friction, rubber-in-shear dampers. Ultimately this design found widespread use in the automotive market due to the satisfactory performance and relatively low cost [5].

In recent years the automotive industry has experienced pressures to reduce fuel emissions and consumption [8]. One method of accomplishing this is to increase engine displacement and reduce cylinder-count and operating speed. For a given power requirement, this requires less fuel which increases average torque, torque pulses, and oscillatory vibration [8]. The automotive industry responded by mounting RPVAs to dual mass flywheels and clutch disks. Advanced RPVA design includes epicycloidal pendulum paths as opposed to circular, trapezoidal pendulum links as opposed to parallel, and end-stop dampers mounted to the pendulum mass instead of the carrier [8]. This represents state-of-the-art RPVA

development. Figure 4 and Figure 5 show some of these design advancements.

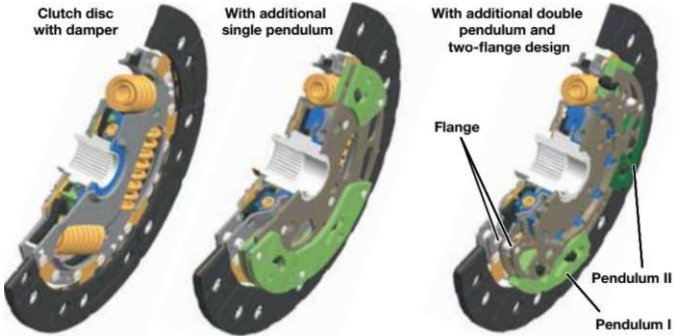


FIGURE 4. CLUTCH DISK WITH & WITHOUT RPVAs [8]

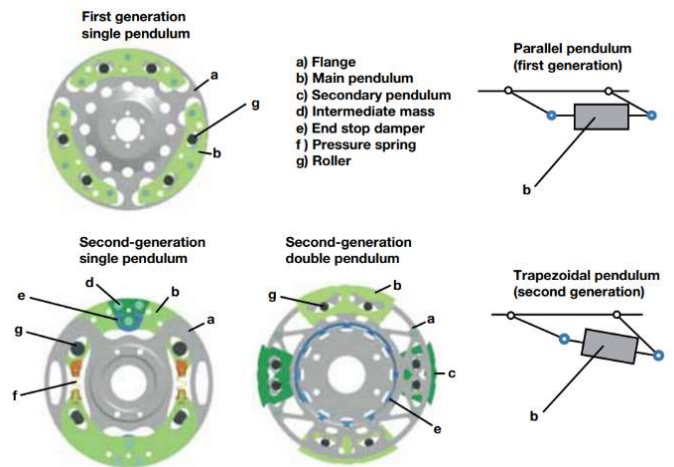


FIGURE 5. EVOLUTION OF CARRIER-MOUNTED RPVA [8]

Various forms of rotating pendulum vibration absorbers are diagrammed in Figure 6. Of the many designs patented in the 1930s and 1940s, those illustrated in Figure 6 are considered the most practical because of their simple mechanical construction [5]. A summary of the designs follows.

Roll Form. Compared to other RPVAs, the active mass of a roll-form RPVA is a much smaller proportion of the total mass of the assembly. However, it is difficult to predict whether the mass will roll or slide on its track while in use. When rolling motion is replaced with sliding, the RPVA's natural frequency is reduced and its performance is impaired.

Bifilar Link Form. In this arrangement, the pendulum mass is connected to the carrier by two links. It is constrained by the links in such a manner that the center of mass will oscillate about an axis midway between the links. The radius of this path is the pendulum's effective length and is solely determined by the length of the links. This makes it easier to add sufficient active mass to the pendulum to keep the pendulum amplitudes low; this is necessary for reliable

performance. Two serious disadvantages accompany the link-form RPVA. Firstly, the hinge pins introduce a large amount of friction into the system and may quickly deteriorate its performance. Anti-friction bearings help solve this problem at the expense of added mechanical complication. Secondly, since the minimum effective pendulum length is determined by the length of the shortest link which may be installed between the pendulum mass and the carrier, there may not be sufficient material between the edges of those surfaces to install hinge pins of adequate size.

Ring Form. This arrangement involves a metal ring which oscillates on a pin fixed to the carrier. Its operation and design problems are similar to those of the roll-form RPVA. Principally, it is difficult to predict whether the mass will slide or roll on its track, or both. The ring-form RPVA is often preferred over the roll-form RPVA because it is more readily accommodated on existing machine components.

Bifilar Suspension. This arrangement is similar to the link-form RPVA; however, it has various advantages. First, only rolling friction occurs between the motion of the absorber mass and the carrier, a result of the hardened pins which connect the two components and carry the centrifugal loads. This is unique in that other designs are concerned with sliding friction between components, or friction introduced by links. Second, the effective pendulum radius may be adjusted to any length by changing the pin's geometry.

Duplex Suspension. A unifilar duplex PA, shown in Figure 6, can be considered half of a bifilar suspension. It is designed such that the pendulum mass is supported by a single pin instead of two. The pin maintains rolling friction with the carrier. Both bifilar and unifilar duplex suspensions have been implemented successfully. Still, bifilar suspensions are generally considered more reliable because their motion is more predictable, particularly during moments of acceleration and retardation [5].

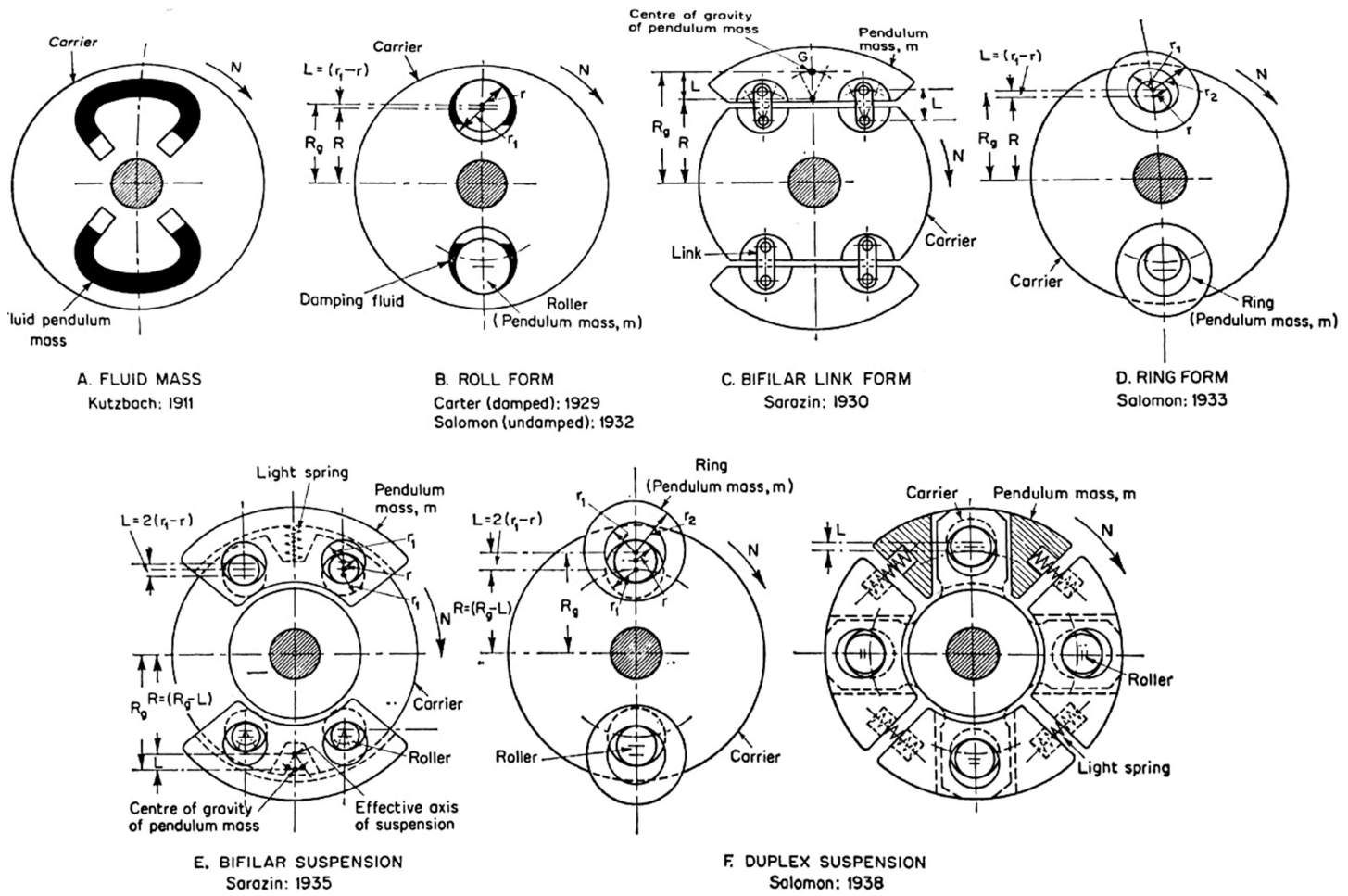


FIGURE 6. VARIOUS FORMS OF ROTATING PENDULUM VIBRATION ABSORBER [5]

1.5 – Project Goals

The client, Spirit Engineering, is looking for a solution to reduce the amplitude of crankshaft torsional vibration by at least 10% by adapting a pendulum absorber to a Kohler CH1000 engine (Figure 1). Therefore, the team has identified five goals to work towards: describe the vibration characteristics and potential vibration reduction of the crankshaft, mass properties of the pendulum assembly, pin radii, angles of rotation, and provide enough design information so the client may conduct a preliminary cost-benefit analysis of employing pendulum absorber(s) into future engine designs. The design information will include the parts involved, geometries, and material. All parts involved shall be capable of operating in a system environment for at least 1000 hours, and the volume of the pendulum must also fit within engine constraints.

1.6 – Validation

The goals for the team center on quantifying crankshaft vibrations and pendulum geometry. Calculation of both depend on outputs from a dynamic model of the crankshaft system. Outputs from the dynamic model are more likely to contain errors than outputs from other project analysis. Therefore, validation of the dynamic model is important to verify the team's goals have been met. If the dynamic model shows crankshaft oscillation magnitudes within +/- 25% of those measured on the physical crankshaft and the predicted engine speed of those oscillations is within +/- 15% of the measured values, the analysis will be considered reliable and valid.

METHODS

The team began their research for the feasibility study by interviewing the client. The client outlined research they had conducted, data and technical resources they had gathered, and goals for the project. The team made note of this information and organized it into project goals, outlined in Section 1.5, and the following eight tasks:

1. Gather RPVA background information
2. Review work done by the client
3. Establish pendulum criteria
4. Select pendulum design based on criteria
5. Create a dynamic model of the system
6. Use Wilson's equations to estimate dynamic model performance
7. Define design boundaries
8. Assess results against project criteria

2.1 - Gather RPVA background information

To gain an understanding of the function and design of pendulum absorbers the team began reviewing videos, technical articles, and historical articles on the subject. Videos were of little use, as content centered on devices that only employed RPVAs as auxiliary mechanisms and did not focus on them specifically. An example of this are dual mass flywheels, which employ RPVAs, but only as a part of a larger solution to vibration issues. Historical articles [6], proved useful in framing the evolution, hurtles, and advantages of pendulums. Technical articles often addressed specific technical improvements or evaluated new applications of pendulum absorbers. They did not, however, fill the need for a comprehensive overview the design process and function of RPVAs. A majority of the technical articles reviewed cited a common source: *Practical Solution of Torsional Vibration Problems* by W. Ker Wilson [4] [5] [7] [9]. Wilson's four volumes on the subject were reviewed extensively by the team and were deemed an invaluable resource.

2.2 - Review work done by the client

One of the team's first priorities was to understand the work already performed by the client. The client performed exploratory tests to visualize and measure the vibration phenomena disturbing the crankshaft with strobe light testing and strain gauges. An understanding of these tests provided project direction by confirming the suspected crankshaft behavior.

One of the first tests aimed to visualize propeller deflection while the engine was running. A strobe light was connected to the engine's magneto so the strobe activated once per revolution. The engine was turned on in a dark room and the strobe light flashed at the same rate as the engine's RPM. Without torsional vibration, the propeller would appear still. During testing, however, the propeller appeared to sway, or rotate, through a small angle. This indicated torsional vibration was occurring within the crankshaft.

To investigate the crankshaft vibration further, the client installed strain gauges on the crankshaft to measure strain while the engine was running. Tests were performed on-ground and in-flight using both the original stock flywheel and the client's custom, lightweight flywheel. Figure shows the location of the installed strain gauges. Each strain gauge recorded instantaneous strain at 3000 to 4000 Hz. Of particular importance to the team was the channel-four strain gauge which measured torsional strain. If this value is known, torsional deflection may then be calculated and used to verify results from calculations and mathematical models.

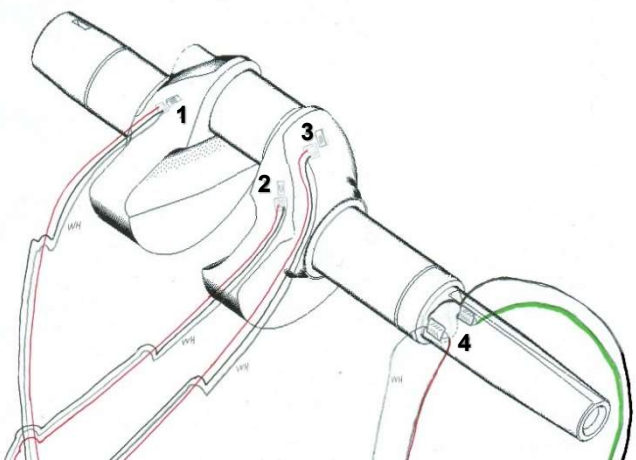


FIGURE 7. LOCATIONS OF STRAIN GAUGES INSTALLED ON THE CRANKSHAFT

The data collected from the channel-four strain gauge indicated resonant conditions occurred, so the natural frequency of the propeller-crankpin-flywheel system was then calculated. Five values must be known to calculate the natural frequency of the system, as presented in Figure . Once these values were calculated, the client used Holzer's method to calculate the natural frequency of a three-mass torsional-spring system.

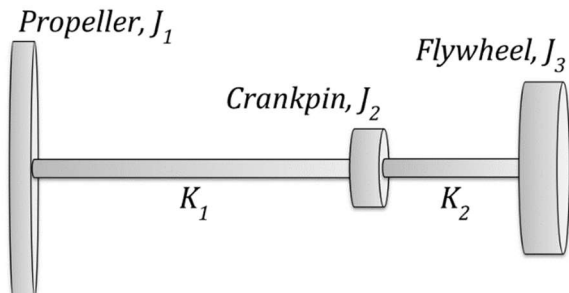


FIGURE 8. DIAGRAM OF THE TORSIONAL SPRING MODEL. J_1 , J_2 , AND J_3 REPRESENT POLAR MOMENTS OF INERTIAS. K_1 AND K_2 REPRESENT SPRING CONSTANTS.

To measure the polar moments of inertia, the propeller and flywheel were separately placed on a device suspended by three strings. The polar moment of inertia was then calculated by measuring the nature of the device's response to a rotational deflection.

The uneven cross-sectional profile of the crankshaft makes calculation of a spring constant difficult, so the shaft was split into be a series of smaller springs with unique geometries. The individual spring constants were then summed to serve as the overall spring constant of the shaft.

2.3 - Establish pendulum criteria

To establish the operating conditions of the RPVA, multiple meetings were held with the client. They provided constraints to the design that were limited by the operation of the aircraft. These included specifications from the engine manufacturer, the range of engine operating speeds, and geometric and weight constraints.

The client provided the team with a crankshaft that had been removed from the Kohler engine. From this, the team created a 3D model of the crankshaft in SolidWorks. This was used to establish constraints such as RPVA geometry and center of mass. Figure 3 shows the counterweight suspended below the crankshaft. The area in blue represents the portion of the counterweight available as RPVA mass. The center of mass of this area was found from SolidWorks and used in subsequent pendulum calculations.

A critical interest of the study concerns the mass of the RPVA. The very motivation to investigate the use of the RPVA is that the potential exists to employ the device without adding weight beyond which is already needed to effectively balance the V-twin engine. Keeping mass to a minimum is a mantra in aircraft design. For this reason, it was decided that the RPVAs shall be mounted to the crank webs of the crankshaft and would be designed such that weight shall not be added to the aircraft in so doing.

2.4 - Select pendulum design based on criteria

Section 1.3 and 1.4 of this report cover the history, function, pros, and cons of RPVAs. Wilson's text [5] in particular was critical to understanding the design of RPVAs. Three points of key importance were identified. First, the pendulum swings about its axis of rotation. The angle which the RPVA swings about this axis is inversely proportional to the mass of the RPVA. This angle is denoted by β in Figure 3. Second, this angle may only be so large before the pendulum no longer functions properly due to the transition from rolling to sliding friction. Third, the magnitude of this angle varies depending on the design of the RPVA [5]. Figure 6 shows the various RPVA designs. The design using bifilar suspension (E) has the most reliable performance of the designs shown. It also has the largest permissible angle of oscillation. This means a smaller pendulum of this design may be used. It is more complex to manufacture than a duplex suspension, making the

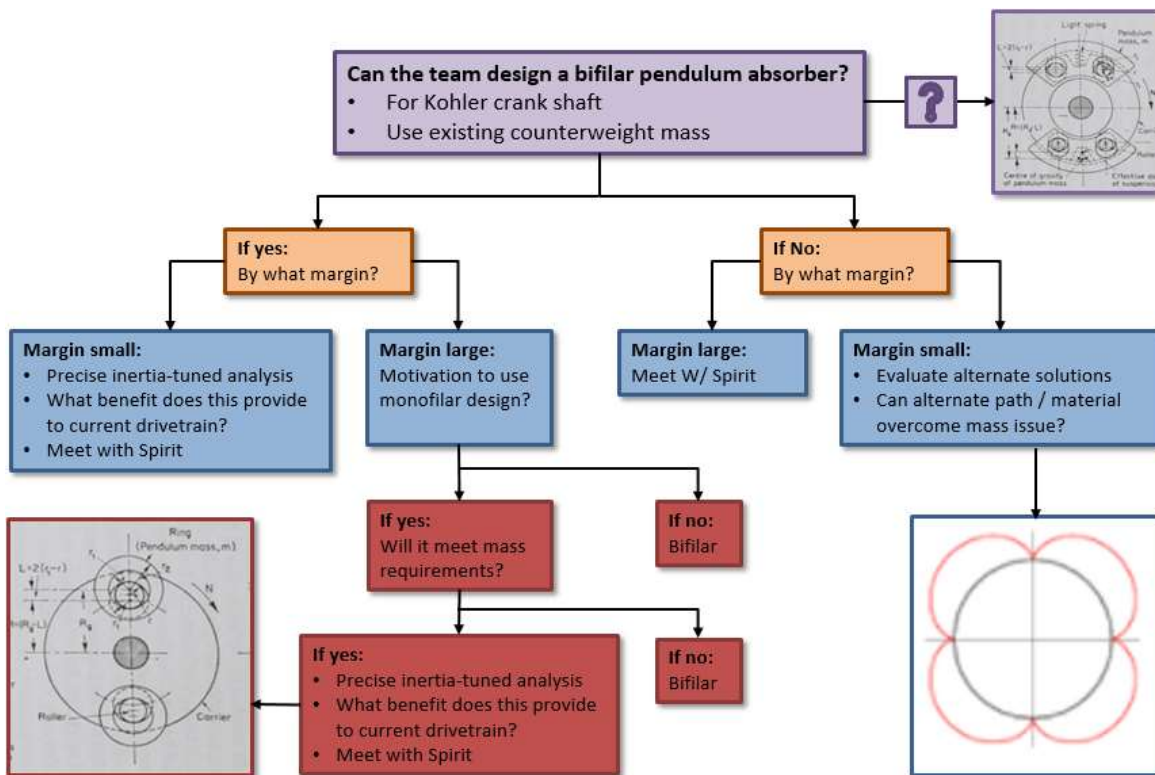


FIGURE 7. PROCESS FLOW CHART

duplex suspension attractive from the standpoint of cost of manufacture.

To choose an appropriate RPVA design, including the type of RPVA suspension, the team created a process flow chart (Figure 7). This illustrates the process of narrowing the design down to that which best fits the project. The first step is to analyze the minimum mass required by a bifilar RPVA. If the mass available in the counterweight exceeds the mass required by the RPVA then the design is feasible. If this is true by a large margin then cost considerations may drive the design into duplex suspension, which is less effective for a given mass, but cheaper to manufacture. If the analysis were to show that not enough mass is available then the right side of the flow chart shows backup solutions that may still make the design feasible. These included more advanced suspension paths that are more difficult to analyze, as well as the use of heavy metals. The latter would make the pendulum more effective for a given weight by increasing the density at key locations. This would increase the cost of the solution.

The minimum mass required by the RPVA was calculated using techniques and equations from Wilson [5]. A generic process for evaluating RPVAs with different input conditions was created by writing a script in MATLAB. The RPVA is tuned to the order that will cause the most harmonic excitation to the crankshaft within the range of operating speeds of the engine. This excitation causes stress to the shaft that may lead to fatigue failure. An input torque, which represents the torque applied to the crankshaft by the crankpin, is imported into the script (Figure). For the sake of simplicity, the torque used in this analysis ignores inertial effects and is based only on force due to piston pressure. The methods in Wilson use the same approximation. This torque is broken into harmonic components using Fourier analysis. The magnitude of the harmonic component of torque to which the RPVA is tuned is found using MATLAB's FFT function, which stands for Fast Fourier Transform. This magnitude is then fed into the pendulum sizing script to obtain the minimum mass required by the RPVA to maintain reliable function.

2.5 - Create a dynamic model of the system

The team's primary analysis tool is a dynamic mathematical model of the system coded in MATLAB. The first step in creating the dynamic model is to define the torsional spring system as a series of three free-floating inertias connected with two torsional springs as shown in Figure . The term free-floating indicates the inertias are not externally fixed and are free to vibrate and accelerate as prescribed by the input torque and damping. The dynamic model is designed to accept torque as a function of time and calculate the relative deflections of the flywheel, crankpin, or propeller.

The team first calculated an input torque by obtaining the torque curve (as percent of mean torque) produced by a single cylinder in a four-stroke-cycle as a function of crankshaft position [9]. Excel was used to create a dataset that matched that of EPI's torque curve. To replicate the V-twin's firing

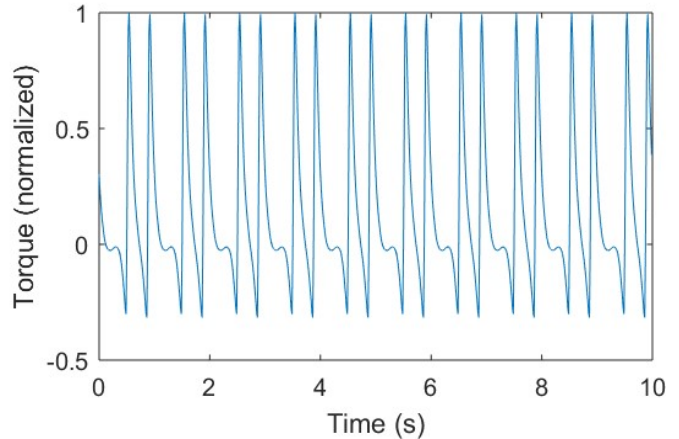


FIGURE 10. PLOT OF TORQUE VS. TIME, AMPLITUDE NORMALIZED FOR SUBSEQUENT CALCULATIONS

order, a duplicate of the data was offset by 270 degrees and summed with the original curve. A MATLAB script was created to obtain the instantaneous torque by multiplying the data by the mean torque and re-calculating the data as a function of time for a given speed. The mean torque was obtained from Kohler's specifications [10] and confirmed with a comprehensive online calculator from [11]. MATLAB's built in differential equation solver, ODE45, was then used to calculate the response of the system.

2.6 - Use Wilson's equations to estimate dynamic model performance

A second approach to calculating the system response was utilized in parallel alongside development of the dynamic model to improve reliability and confidence of the results. Volumes 1-4 Wilson's text describes the nature of vibrating systems, outlines methods for analyzing multiple-mass systems, and provides calculations to implement pendulum absorbers into existing models. Note that this approach doesn't output a temporal dataset like the dynamic model. In other words, instantaneous amplitudes cannot be observed. However, Wilson's methods provide peak deflection amplitudes for each order of vibration at their respective critical speed.

The team implemented Wilson's methods [12] in MATLAB, to calculate the system's natural frequencies and relative deflections. Similarly, Volume 2 of Wilson's texts [4] guided vibration amplitude calculations for each inertia at a selected speed. A Fourier analysis of the input torque was performed to obtain the amplitudes and frequencies, or orders, of the sin waves that compose it. Figure 8 displays part of the Fourier transformation.

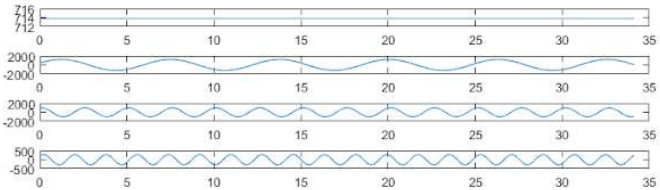


FIGURE 8. THE FIRST FOUR COMPONENTS OF THE INPUT TORQUE OBTAINED FROM A FOURIER TRANSFORMATION. AMPLITUDE (IN LBS) AS A FUNCTION OF CRANK ANGLE (RADIAN).

For each component of the torque, a series of calculations were performed to obtain the crankshaft's response at a given speed. These calculations were repeated over the engine's range of operating speeds so the peak amplitudes of each order and their critical speed may be compared.

The model was used in conjunction with excel datasets corresponding with four different engine tests. Each test utilized flywheels with different inertia values. This provided vibrations amplitudes over an RPM sweep for four different system configurations. The four datasets/configurations are identified by the flywheel used, from lightest to heaviest: überlight, Spirit, weighted Spirit, and the Kohler flywheel. The Kohler and Spirit dataset were used to tune the system, while the überlight and weighted Spirit dataset were used to verify model predictions.

Major assumptions of this approach include the use of constant peak torque values over all engine speeds, internal damping coefficients of the crankshaft, and a pendulum absorber tuned exactly to the fourth order.

2.7 - Define Pendulum Design

The team does not bear the responsibility of creating the final pendulum design for this project. Concerns regarding the interplay between manufacturing costs, reliability, and design are beyond the scope of this project. There are certain parameters of the design regarding geometries, suspension style, and strength that must be met for the RPVA to function properly. The team is responsible for defining these parameters and providing them to the client.

In addition, the team was tasked with creating a 3D model of the crankshaft and an RPVA. The crankshaft model is used for various aspects of analysis in the project, so its accuracy is of utmost importance. The RPVA model is only used to aid in communicating the function and principal of the RPVA and therefore was not held to strict geometric tolerance. Both were modeled in SolidWorks. The client provided the team with a crankshaft that had been removed from the Kohler engine. The team measured the geometry of this crankshaft to create a 3D model.

The team determined an RPVA using bifilar suspension should be used for this project. The Results section of the report supports this choice. The four essential components of a bifilar RPVA include the pendulum mass, carrier, pin, and track. Figure 6 shows a line drawing of these components. Figure 9 shows a potential bifilar RPVA model adapted to the Kohler

crankshaft. It is essential that the geometry of the pin, track, and center of mass of the pendulum is tightly controlled. These geometries determine the order to which the pendulum is tuned. Methods from Wilson [5] were adapted into a MATLAB script to determine these geometries as well as the line contact stress between the tracks and pin. This allowed multiple configurations to be investigated rapidly. Geometry calculations also had to be adapted from a roll-form RPVA to a bifilar RPVA.

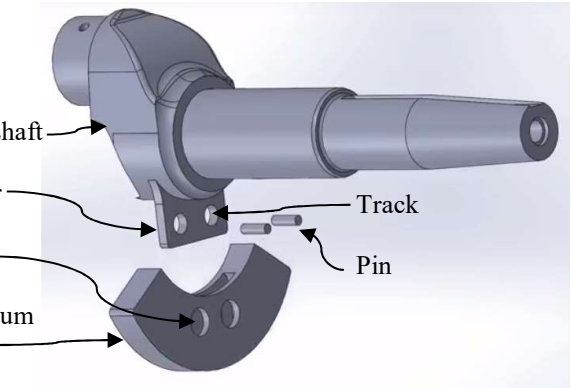


FIGURE 9. BIFILAR RPVA ON KOHLER CRANKSHAFT

2.8 - Assess results against project criteria

To find a solution of reducing amplitude torsional vibrations, the team introduced five project goals, outlined in section 1.5. The first goal is the cynosure that drives the project forward while the others are used to support it. Finding the amount of reduction began by: assembling a dynamic model in MATLAB using an inertia model, generating a torque curve to model the input torque produced by the engine, and performing calculations on pendulum absorbers outlined by Wilson. All calculations are calculated in an array over time, or samples, from the four different sets of strain gage data. These arrays produce graphs showing specific vibrational orders and the amount each order interacts with the system. Tuning a pendulum absorber to most harmful excitation reduces the amount of amplitude torsional vibrations.

The remaining goals followed similar processes as described above by using MATLAB along with methods and calculations described by Wilson [5] to calculate the minimum mass required, track and pin radii, and the amount of angular oscillation. The team was unable to provide physical verification because designing the pendulum absorber was out of the project scope.

RESULTS

The Results section presents the most important findings from Task 2 through Task 8.

3.2 - Review work done by the client

The client affixed strain gauges to the crankshaft as diagrammed in Figure to explore how various flywheel configurations effected vibrations. A change to the flywheel geometry affects the mass moment of inertia of the flywheel and the resonant frequency of the dynamic system. This has the effect of changing where along the power-band a harmonic component of torque aligns with the natural frequency of the system. Torsional strain is shown in **Error! Reference source not found.**, **Error! Reference source not found.**, and **Error! Reference source not found.**. These figures show the strain at the crankshaft from speeds just above idle (1,700 rpm +/-) to wide open throttle (WOT).

An analysis of **Error! Reference source not found.** shows that the natural frequency of the Kohler flywheel is 162 Hz. The location of the 4th order of harmonic input torque aligns early within the power-band for this system. Resonant

conditions are shown for the 4th order just after idle. The amplitude, 390 $\mu\text{in/in}$, is similar to orders 3.5 and 3.

Error! Reference source not found. shows that with the lightweight Spirit flywheel, the resonant frequency is now 218 Hz. The 4th order resonance has shifted toward WOT. It is not fully developed at WOT, but shows an amplitude 44% higher than the Kohler flywheel, 560 $\mu\text{in/in}$.

The two previous tests were run on the ground. The aircraft was held stationary relative to the air-mass surrounding it. In flight the aircraft has a velocity relative to the air-mass in which it is flying. This has the effect of unloading the propeller and engine, allowing the crankshaft to reach higher angular velocity. To simulate this condition, the client added a lower-pitch propeller. **Error! Reference source not found.** shows the lightweight flywheel and low-pitch propeller. 4th-order resonance is now fully developed near WOT. The amplitude, over 700 $\mu\text{in/in}$, is much larger than the case of the Kohler flywheel. The amplitude is also much larger relative to neighboring, higher, orders of harmonic excitation. This data is representative of the conditions when the crankshaft failed in flight at WOT.

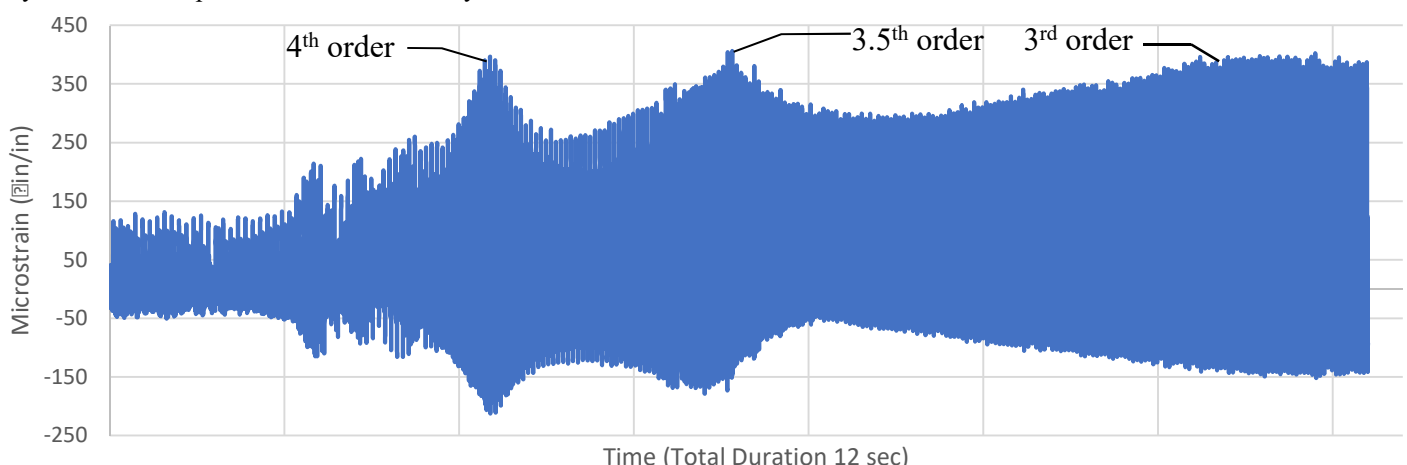


FIGURE 11. ENGINE SPEED SWEEP - IDLE TO WOT, 48 X 32 PROP, KOHLER FLYWHEEL [13]

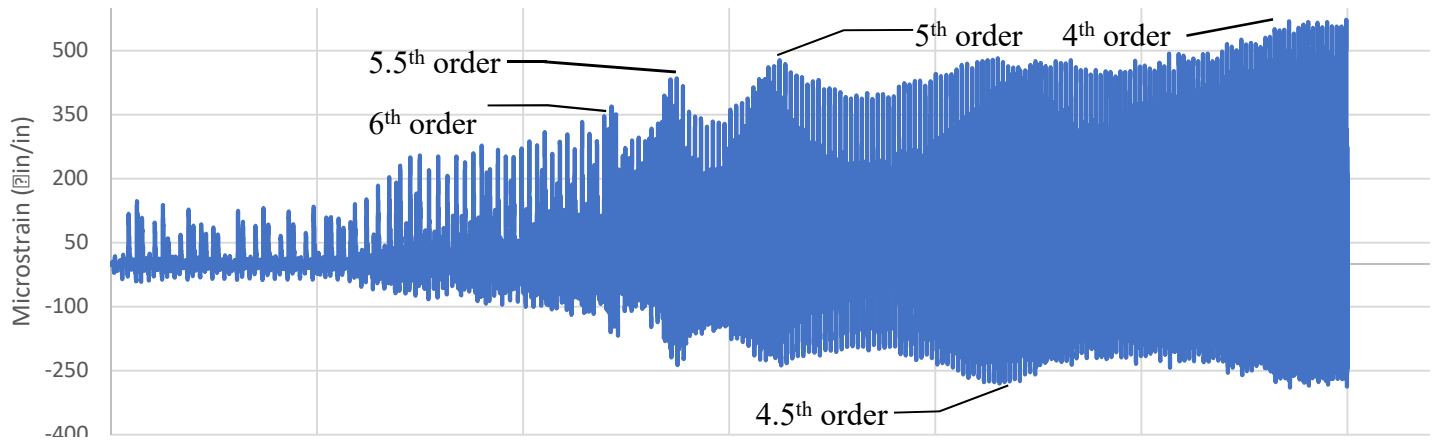


FIGURE 10. ENGINE SPEED SWEEP - IDLE TO WOT, 48 X 32 PROP, SPIRIT FLYWHEEL [13]

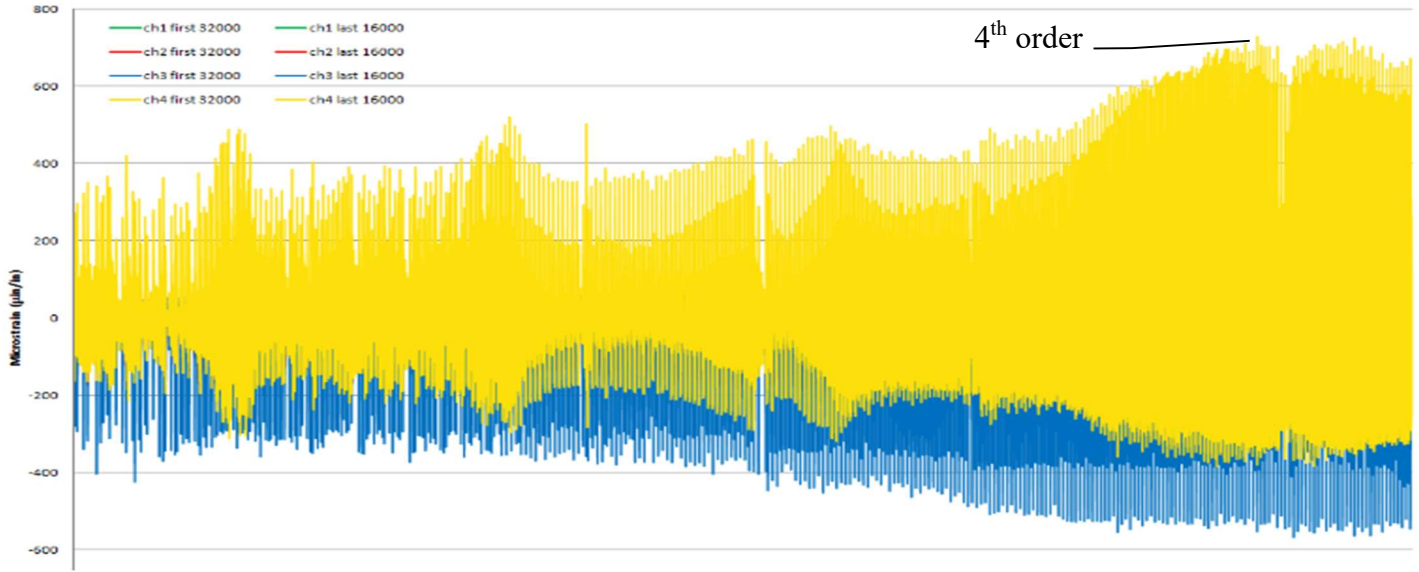


FIGURE 12. ENGINE SPEED SWEEP - IDLE TO WOT, 48 X 22 PROP, SPIRIT FLYWHEEL [13]

3.3 - Establish pendulum criteria

The pendulum must be able to withstand the power generated from the Kohler engine over the operational speed range of the engine. Figure 13 shows a plot of torque vs. engine speed for the Kohler CH100 published by Kohler. The published data does not show torque near idle rpm. The team extrapolated these values using a second order polynomial fit as shown by the blue line.

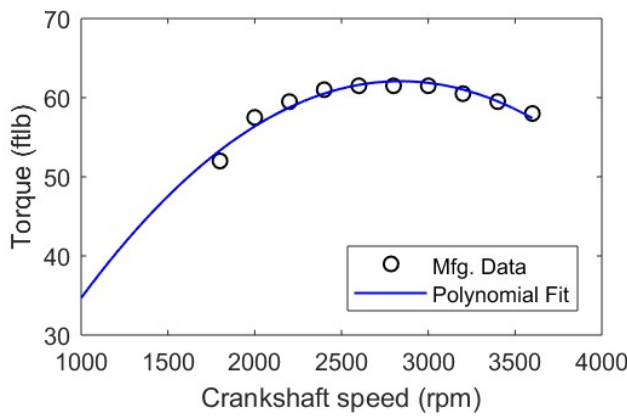


FIGURE 13. PLOT OF KOHLER CH100 TORQUE CURVE VERSUS ENGINE SPEED

The maximum engine operating speed occurs during a full throttle dive. The client determined this to be 3,700 rpm. Other noteworthy engine speeds include climb at 3,300 rpm, cruise at 3,400 rpm, and idle at 1,000 rpm.

The RPVA must fit within the space allotted by the Kohler crankshaft counterweight. It must not interfere with the Kohler crankcase. Figure 14 shows a CAD model of the Kohler crankshaft that the team developed. The team determined from this model that 3.1 lbm of counterweight mass is available to act as the pendulum carrier and pendulum assembly.

The RPVA must function without visual inspection until the engine is overhauled. Time before overhaul was estimated to be 1,000 hours for this project. Pendulums that last the life of the crankshaft are referenced in Wilson [5]. Wilson suggests using carbon case-hardened steel tracks and carbon case-hardened and pins with a tensile strength between 40 and 60 ksi. Wilson recommends limiting line contact stress to 20 ksi where practical and 40 ksi where weight reduction is the ultimate priority. The team determined that line contact stress between the pin and track would need to be limited to less than 40 ksi.

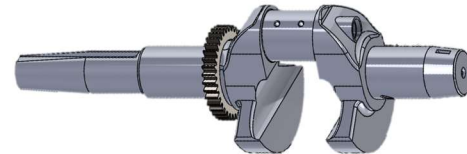


FIGURE 14. CAD MODEL OF KOHLER CRANKSHAFT

3.4 - Select pendulum design based on criteria

Figure shows a generic normalized torque curve the team constructed for a 90-degree V-twin engine. The harmonic components of this curve are shown in Figure 15. The fourth-order component of this torque much lower than the total torque, roughly 5%. Depending on the shape of the curve the bifilar RPVA mass required to counteract this torque was

calculated between 0.22 and 0.33 lbm. Because of the uncertainty in this mass calculation, the desire to operate the pendulum with an oscillation of 20 degrees instead of 25 degrees, and typical structural safety factors in aircraft of 1.5, a final safety factor of 3 was used for the estimate of the maximum pendulum mass required for the project. This gives a pendulum mass of 1.0 lbm.

If the assumption is made that half of the counterweight mass is available as the pendulum, and the other half will count as the carrier, then 1.55 lbm is available as pendulum mass. This is more than the required 1.0 lbm, but not by a large margin. Figure 7 shows a bifilar RPVA will be selected if the required margin of mass is small. Bifilar pendulums use their available mass more effectively than other designs because of where the mass is positioned. They will also maintain stable operation through 25 degrees of oscillation, 5 degrees more than the next most effective design. Anecdotally, bifilar pendulums operate more reliably and oscillation behavior is predicted more reliably by models than other designs [5].

Direct shear limits the diameter of the pin to 0.14 in diameter for a shear stress of 11.6 ksi. The team determined that line contact stress between the pin and track of a bifilar RPVA is 14 ksi for a track of 0.2 in radius, this is less than the required maximum of 40 ksi, making the pin and track configuration feasible.

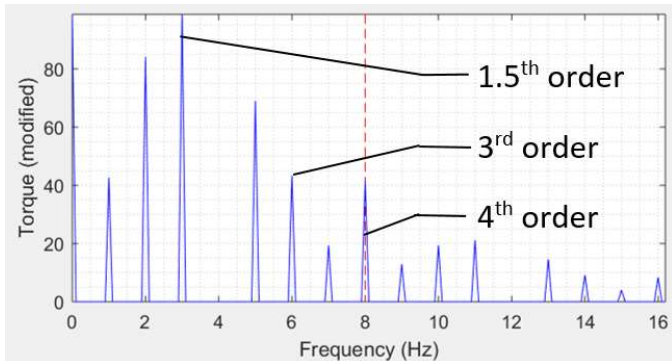


FIGURE 15. HARMONIC COMPONENTS OF INPUT TORQUE

3.5 - Create a dynamic model of the system

The mathematical model of the spring system is shown in Appendix 2. The input torque that was constructed from EPI's data is shown in Figure 16. This torque curve was summed with the same curve 270 degrees out of phase to create the plot shown in Figure . This curve was scaled, depending on engine speed, by the curve shown in Figure 13. This final curve is shown in Figure 17. This is the input torque that was used in the dynamic system model.

The dynamic system model output is shown in Figure 18. The expectation was to see response of similar shape to the plot of strain vs. sample number shown in Figure 17. Since this was not the case, a test of the model's response to resonance was run

by using a pure sine wave of increasing frequency as the torque input. The model did not show increased displacement at locations of harmonic resonance (Figure 19).

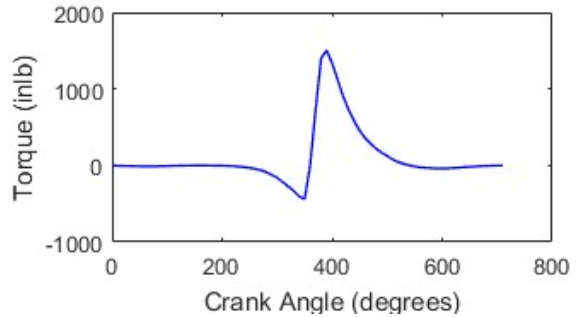


FIGURE 16. PLOT OF TORQUE VS. CRANK ANGLE FOR A SINGLE CYLINDER COMBUSTION ENGINE

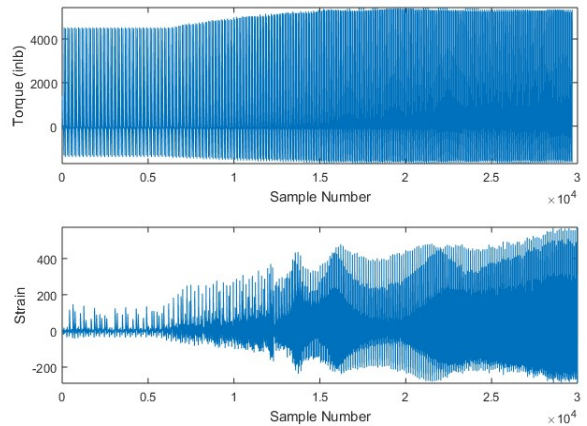


FIGURE 17. PLOT OF INPUT TORQUE VS SAMPLE NUMBER (TOP) AND MEASURED STRAIN VS. SAMPLE NUMBER (BOTTOM)

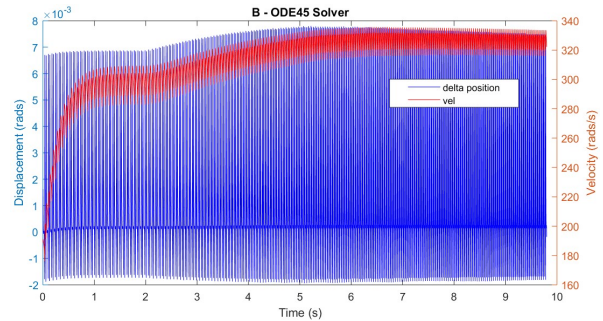


FIGURE 18. DYNAMIC SYSTEM OUTPUT – PLOT OF DISPLACEMENT VS. TIME – INPUT TORQUE FROM FIGURE 17

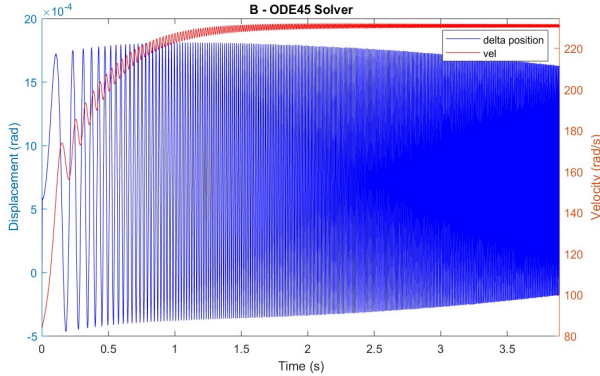


FIGURE 19. DYNAMIC SYSTEM OUTPUT – PLOT OF DISPLACEMENT VS. TIME – INPUT TORQUE AS A PURE SIGN WAVE OF INCREASING FREQUENCY

3.6 - Use Wilson's equations to estimate dynamic model performance

The secondary mathematical model defined by Wilson's methods generated a series of plots describing the system. The Spirit and Kohler datasets were used as guidelines to tune the amplitude predictions. MATLAB was used to adjust the amplitudes of the 3rd, 3.5th, 4.5th, and 5th order sine wave inputs to match the prediction's amplitudes with the observed values. Figure 20 shows each order's amplitude prediction for the Kohler system before and after adjusting the inputs.

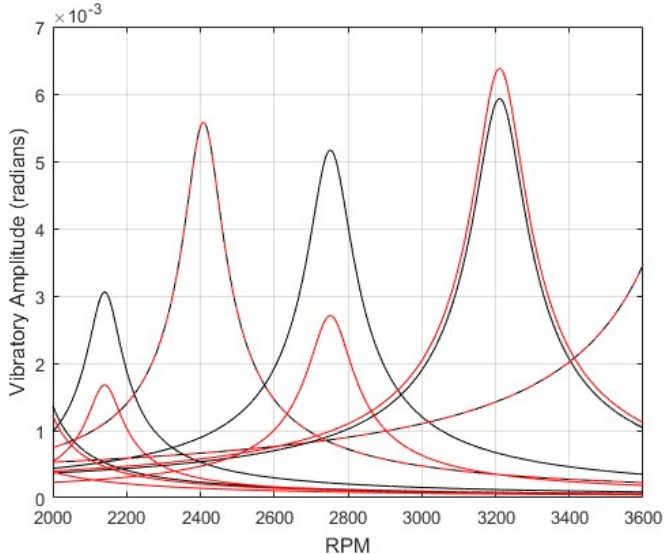


FIGURE 20. KOHLER SYSTEM – ADJUSTED AMPLITUDES PREDICTIONS (BLACK)

The model was used in conjunction with datasets corresponding to the different flywheel configurations used in testing. Table 1 summarizes each flywheel's inertia (J_3) and natural frequencies (ω_{nf}). The adjusted J_3 is the required value for Wilson's ω_{nf} calculations to match the observed ω_{nf} . Figure 24 shows how each peak changes when the inertia is changed.

TABLE 1. INERTIA VALUES AND NATURAL FREQUENCIES OF EACH SYSTEM

System Name	Measured J_3	Adjusted J_3	Observed ω_{nf} (Hz)
Überlight	0.094	0.153	253
Spirit	0.163	0.263	217
Weighted Spirit	0.438	0.438	187
Kohler	0.857	0.8025	161

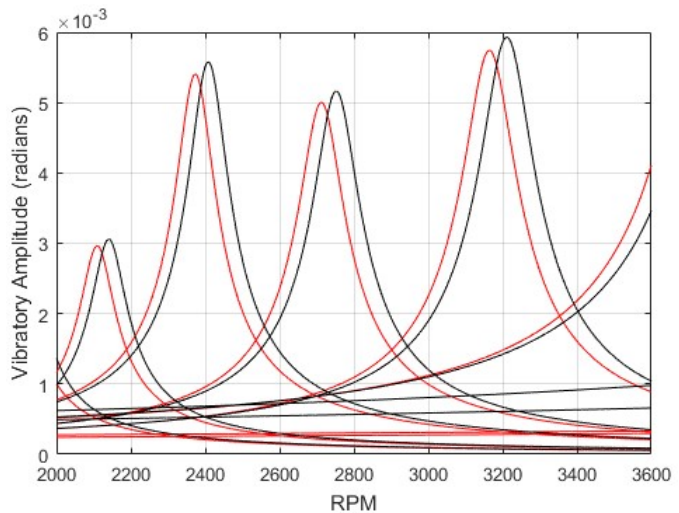


FIGURE 21. KOHLER SYSTEM - AMPLITUDE PREDICTION USING MEASURED J_3 (RED) AND ADJUSTED J_3 (BLACK)

Figure 23 and Figure 22 show comparisons between the amplitude predictions and the observed data for the Kohler and Spirit System. The predictions use the adjusted J_3 values. The amplitudes of the predictions were tuned using their respective observational data. Note that the predicted amplitudes are less than the observed values. Note the observational data were recorded as a function of sample number and the x-axis are not the same between plots. Peaks are labeled with their corresponding RPM and order number.

Figure 25 and **Error! Reference source not found.** compare the amplitudes between the predicted and observed values for the überlight and weighted Spirit system. The predicted values were calculated after tuning the model using Figure 23 and Figure 22. In both cases the predicted amplitudes matched the relative amplitudes and form of the observed data.

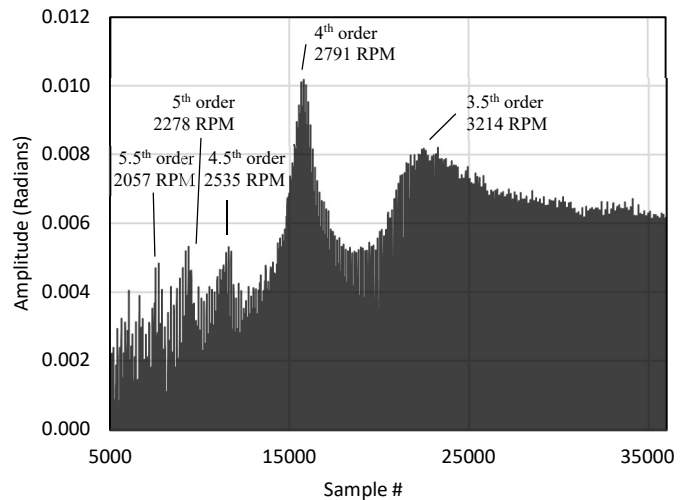
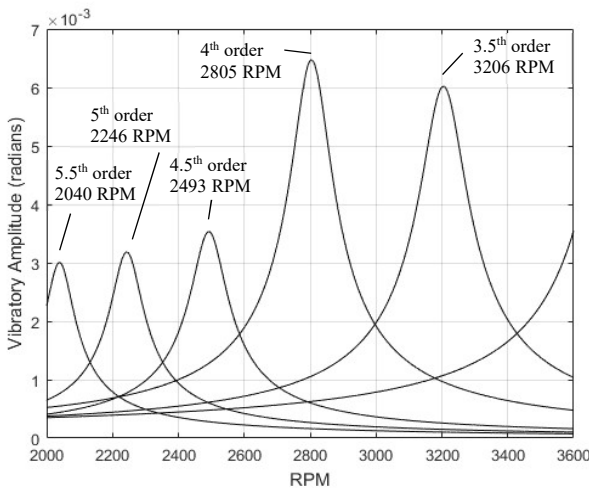


FIGURE 24. WEIGHTED SPIRIT SYSTEM (VERIFICATION) – AMPLITUDE COMPARISON BETWEEN PREDICTIONS (LEFT) AND OBSERVATIONS (RIGHT)

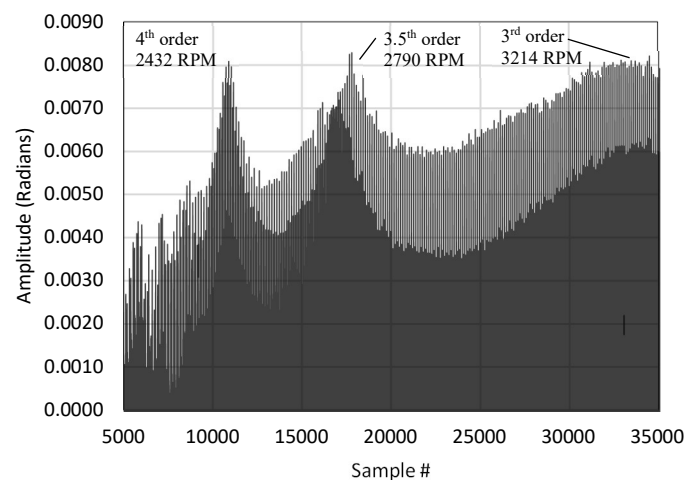
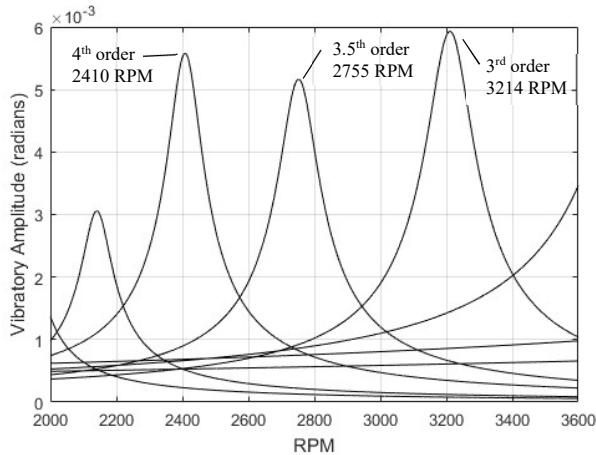


FIGURE 23. KOHLER SYSTEM (TUNING) – AMPLITUDE COMPARISON BETWEEN PREDICTIONS (LEFT) AND OBSERVATIONS (RIGHT)

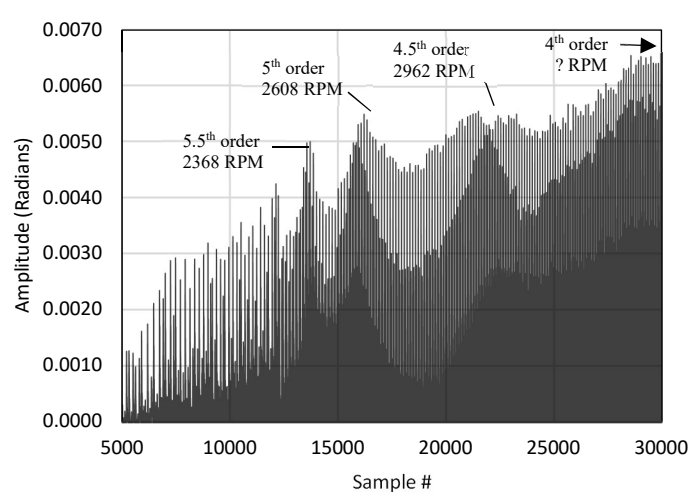
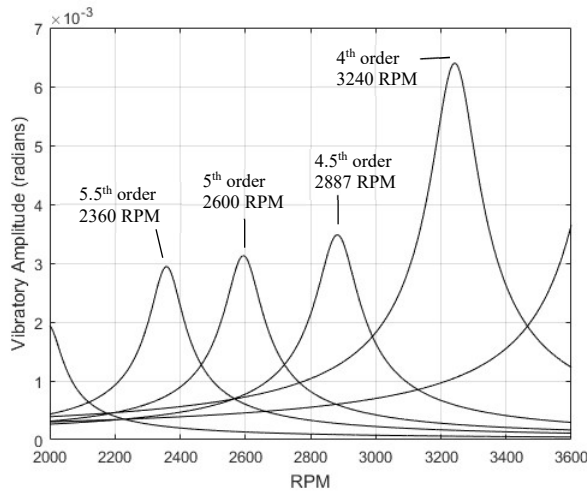


FIGURE 22SPIRIT SYSTEM (TUNING) – AMPLITUDE COMPARISON BETWEEN PREDICTIONS (LEFT) AND OBSERVATIONS (RIGHT)

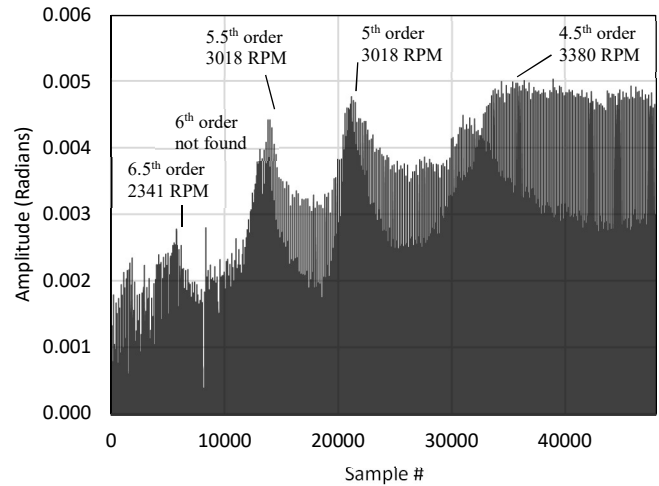
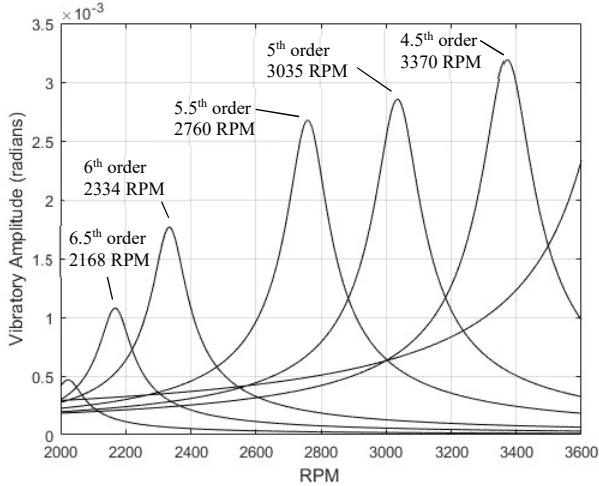


FIGURE 25. UBERLIGHT SYSTEM (VERIFICATION) – AMPLITUDE COMPARISON BETWEEN PREDICTIONS (LEFT) AND OBSERVATIONS (RIGHT)

3.7 - Define Pendulum Design

For a bifilar RPVA to function properly, the geometry of the suspension must be accurately defined. The team developed a formula for relating the pin and track geometry based on rules observed in Wilson [5]

$$r = r_1 - \frac{R_g}{2(n^2 + 1)} \quad (1)$$

where r is the radius of the pin, r_1 is the radius of the track, R_g is the distance from the axis of rotation of the carrier to the center of mass of the pendulum, and n is the order to which the pendulum is tuned. This may be used to design any bifilar RPVA.

For the case of the Kohler crank, R_g was measured at 2.00 in. If a radius of 0.200 is chosen for the track, then the pin must be 0.141 in in diameter. Other combinations of pin and track radius will work as long as Equation 1 is adhered to and structural stresses are not exceeded.

3.8 - Assess results against project criteria

The client sponsored this project to determine if adapting an RPVA to a Kohler CH1000 engine (Figure 1) could reduce the amplitude of crankshaft torsional vibration by at least 10%. The team determined that they needed to meet five project goals to accomplish this:

- 1 Quantify the reduction in crankshaft oscillation if an RPVA were employed
- 2 Determine the mass of the RPVA
- 3 Determine pin and track radii
- 4 Determine the angle of oscillation of the RPVA
- 5 Provide enough design information so the client may conduct a preliminary cost-benefit analysis of employing pendulum absorber(s) into future engine designs.

Goal one was met. Figure 26 shows that 54% of the crankshaft oscillation would be removed from the Kohler crankshaft with the Kohler flywheel mounted. This is well above the minimum desired reduction of 10%.

Goals 2 and 3 were met. The RPVA mass was determined to be 1 lbm and pin and track radii were determined to be 0.141 in and 0.200 in respectively. Goal 4 was met, the maximum RPVA oscillation was determined to be 20 degrees.

Goal 5 was met. Goals 2 through 4 describe the physical geometry of the RPVA. Additionally, Section 3.3 of the report outlines pin and track strength and material requirements and emails were sent to the client outlining common bifilar pendulum arrangements.

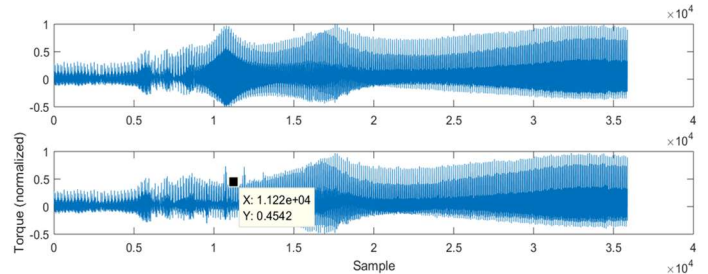


**FIGURE 26. PLOT OF NORMALIZED TORQUE VS. SAMPLE FROM SPIRIT STRAIN-GAGE DATA (TOP)
PREDICTED NORMALIZED TORQUE VS. SAMPLE WITH
4TH ORDER PENDULUM IN SYSTEM (BOTTOM)**

The client is interested in future engine designs other than the Kohler CH1000. If Goals 1-5 are to be met for a future engine design, one where crankshaft strain-gage data was not available, then this data would have to be obtained from predictive models. The team developed two models for this purpose. It was determined that two criteria needed to be met for these models to be considered valid:

1. The model shows crankshaft oscillation magnitudes within +/- 25% of those measured on the physical crankshaft
2. The model predicts engine speeds of those oscillations within +/- 15% of the measured values

The dynamic model failed both of these criteria. The error was so large that there was no discernable resemblance between predicted and measured system behavior.

The model developed using Wilson's methods generated amplitude predictions comparable with observational data. Since the systems' natural frequencies were tuned using inertia values, the locations of the critical speeds were adjusted to match that of the observed data. The magnitude of vibration predictions were also within +/- 25% of those measured on the physical crankshaft.

CONCLUSION

In this section, the team presents conclusions based on research related to project goals and tasks. Computational analysis using MASTLAB and Wilson's methods of RPVA design led to the following conclusions: 54% of the fourth-order oscillation would be removed from the crankshaft with the Kohler stock flywheel attached. An RPVA mass of one lbm, with 20 degrees of oscillation, track radii of 0.141 in, and pin radii of 0.200 in will provide the 54% reduction in the fourth-order oscillation.

The method of analyzing the crankshaft dynamic system, as outlined in Section 2.5, does not provide reliable output. This method should be improved or abandoned in figure work.

Following Section 2.6, Wilson's methods do provide useful predictions of amplitude and location of resonant conditions. With amplitude predictions, crankshaft strain and fatigue life may then be calculated. However, this approach is only useful when paired with data for tuning the model. The deflection amplitudes, and even the relative amplitudes between orders, may not be verified without test data.

BIBLIOGRAPHY

- [1] J. Zimmerman, "The Great Debate: Is The LSA Rule A Failure?," *Air Facts the journal for personal air travel- by pilots, for pilots*, 2012.
- [2] Kohler Co., "Kohler Command PRO CH940-CH1000 Service Manual," [Online]. Available: http://www.kohlerengines.com/onlinecatalog/pdf/62_690_01_EN.pdf.
- [3] L. T. S. Z. Y. Xiaoyong, "Numerical analysis and improvement of torsional vibration of shaft systems for engine with cylinder deactivation," *Computer Modeling & New Technologies*, vol. 18, no. 2, pp. 76-82, 2014.
- [4] W. K. Wilson, Practical Solution of Torsional Vibration Problems, 3 ed., vol. 2, Chapman & Hall, 1963.
- [5] W. K. Wilson, Practical Solution of Torsional Vibration Problems, 3 ed., vol. 4, Chapman & Hall, 1968.
- [6] K. D. McCutchen, "No short days: The struggle to develop the R-2800 "Double Wasp" crankshaft," *American Aviation Historical Society Journal*, vol. 46, no. 2, pp. 124-146, 2001.
- [7] W. K. Wilson, Practical Solution of Torsional Vibration Problems, 3 ed., vol. 3, Chapman & Hall, 1965.
- [8] A. Kooy, "The Evolution of the Centrifugal Pendulum-Type Absorber not only for the DMF".
- [9] W. K. Wilson, Practical Solution of Torsional Vibration Problems, 3 ed., vol. 1, Chapman & Hall, 1956.
- [10] EPI Inc., "Torsional Output of Piston Engines," 14 March 2017. [Online]. Available: http://www.epi-eng.com/piston_engine_technology/torsional_excitation_from_piston_engines.htm. [Accessed 11 2018].
- [11] Kohler Co., "Command Pro CH1000," [Online]. Available: <http://www.kohlerengines.com/onlinecatalog/productDetail.htm?productNumber=Command%20PRO%20CH1000>. [Accessed 11 2018].
- [12] HPWizard, "Estimating Engine Power," [Online]. Available: <http://hpwizard.com/engine-horsepower-calculator.html>. [Accessed 11 2018].
- [13] E. S. Taylor, "Eliminating Crankshaft Torsional Vibration in Radial Aircraft Engines," *SAE International*, vol. 38, no. 3, March 1936.
- [14] C. Taylor, The Internal-Combustion Engine in Theory and Practice: Combustion, Fuels, Materials, Design, Revised ed., vol. 2, Cambridge, Massachusetts: The M.I.T. Press, 1985.
- [15] V. Simmianatto, "<https://drive.google.com/file/d/0BymUQYzMN1xFSkdMdUU2VEE0UVU/view>," University of Campinas, 2015.
- [16] A. Y. V. Londhe, "Design and Optimization of Crankshaft Torsional Vibration Damper for a 4-Cylinder 4-Stroke Engine," *Load Simulation and Analysis in Automotive Engineering*, 2008.
- [17] H. H. Denman, "Tautochronic Bifilar Pendulum Torsion Absorbers for Reciprocating Engines," *Journal of Sound and Vibration*, vol. 159, no. 2, pp. 251-277, 1 August 1991.
- [18] M. A. Acar, "Design and Turning of Centrifugal Pendulum Vibration Absorbers for Nonlinear Response," 2017.
- [19] "Piston Motion Basics," 08 August 2014. [Online]. Available: http://www.epi-eng.com/piston_engine_technology/piston_motion_basics.htm. [Accessed 28 09 2017].
- [20] EPI Inc., "Crankshaft Torsional Absorbers," 3 July 2014. [Online]. Available: http://www.epi-eng.com/piston_engine_technology/crankshaft_torsional_absorbers.htm. [Accessed 28 09 2017].

APPENDIX 1 – MATHEMATICAL MODEL OF DYNAMIC SYSTEM

Resonance 4

FIND:

Pin \in Track radii for resonance tuning.

GIVEN:

$$n^2 L = R \quad \text{for resonant condition} \quad (\sum j_{en} = +\infty) \quad \text{Pg. 556}$$

$$L = L_{eq} = 2(r_i - r), \quad R = Pg - L \quad \text{Pg. 562}$$

SOLUTION:

Assume Pg, r_i, n are known

$$n^2 L = R = Pg - L \Rightarrow L = \frac{Pg}{n^2 + 1} = 2(r_i - r) \Rightarrow$$

$r_i - \frac{Pg}{2(n^2 + 1)} = r$

SKETCH:

APPENDIX 2 – MATHEMATICAL MODEL OF DYNAMIC SYSTEM

3-0235 – 50 SHEETS – 5 SQUARES
 3-0236 – 100 SHEETS – 5 SQUARES
 3-0237 – 200 SHEETS – 5 SQUARES
 3-0137 – 200 SHEETS – FILLER

Dynamic System | Kohler | Prop

Assume $\dot{\theta}_2 > \dot{\theta}_1, \dot{\theta}_2 > \dot{\theta}_3$

03/06/18 2

COMET

$F = MA \Rightarrow \Sigma T = I \ddot{\theta}$

Neglect Inertia from shaft

$\uparrow \leftarrow \downarrow \quad \uparrow \uparrow \quad \uparrow \uparrow \quad \uparrow \uparrow$

$$T_2 - K_a(\theta_2 - \theta_1) - K_b(\theta_2 - \theta_3) - C_a(\dot{\theta}_2 - \dot{\theta}_1) - C_b(\dot{\theta}_2 - \dot{\theta}_3) = I_2 \ddot{\theta}_2$$

$$-T_3 + K_b(\theta_2 - \theta_3) + C_b(\dot{\theta}_2 - \dot{\theta}_3) = I_3 \ddot{\theta}_3$$

$$K_a(\theta_2 - \theta_1) + C_a(\dot{\theta}_2 - \dot{\theta}_1) = I_1 \ddot{\theta}_1$$

$$I_2 \ddot{\theta}_2 + \dot{\theta}_2(C_b + c_a) + \theta_2(K_b + K_a) = \dot{\theta}_1 C_a + \dot{\theta}_3 C_b + \theta_1 k_a + \theta_2 k_b + T_2$$

- Stable -, may use S.V. form for ODE

$$I_3 \ddot{\theta}_3 + \dot{\theta}_3(C_b + C_{T_3}) + \theta_3 K_b = \dot{\theta}_2 C_b + \theta_2 k_b - T_3, \quad \text{stable}$$

$$I_1 \ddot{\theta}_1 + \dot{\theta}_1 C_a + \theta_1 k_a = \dot{\theta}_2 C_a + \theta_2 k_a, \quad \text{stable}$$

Example of S.V. Form – pg. 263

SPINN = 2125 Hz
SPIDE = 165 Hz

Dyn. Sys	Kohler	3
S.V. form - Pg 263 \Rightarrow , ODE- Pg 285.		
$\ddot{\theta}_2$ let $\theta = \theta$, $\dot{\theta} = \phi$, $\ddot{\theta} = \ddot{\phi}$ \Rightarrow	$\begin{bmatrix} \dot{\theta}_1 \\ \dot{\theta}_2 \\ \dot{\theta}_3 \end{bmatrix} = \begin{bmatrix} 0 & 0 & 0 & 0 & 1 & 0 & 0 \\ 0 & 0 & 0 & 0 & 0 & 1 & 0 \\ 0 & 0 & 0 & 0 & 0 & 0 & 1 \end{bmatrix} \begin{bmatrix} \theta_1 \\ \theta_2 \\ \theta_3 \\ \phi_1 \\ \phi_2 \\ \phi_3 \end{bmatrix}$ $= \begin{bmatrix} 0 \\ \frac{-ka}{I_1} & \frac{ka}{I_1} & 0 & -\frac{ca}{I_1} & \frac{ca}{I_1} & 0 \\ \frac{ka}{I_2} & 0 & -\frac{(kb+ka)}{I_2} & \frac{kb}{I_2} & \frac{ca}{I_2} & -\frac{(c_b+c_a)}{I_2} & \frac{cb}{I_2} \\ 0 & \frac{kb}{I_3} & -\frac{kb}{I_3} & 0 & \frac{cb}{I_3} & -\frac{(cb+c_{T_3})}{I_3} & \frac{c_{T_3}}{I_3} \end{bmatrix} \begin{bmatrix} \theta_1 \\ \theta_2 \\ \theta_3 \\ \phi_1 \\ \phi_2 \\ \phi_3 \end{bmatrix}$ $+ \begin{bmatrix} 0 \\ 0 \\ 0 \\ 0 \\ 0 \\ \frac{1}{I_2} \end{bmatrix} \begin{bmatrix} \ddot{\theta}_2 \end{bmatrix}$	

3-0235 — 50 SHEETS — 5 SQUARES
 3-0236 — 100 SHEETS — 5 SQUARES
 3-0237 — 200 SHEETS — 5 SQUARES
 3-0137 — 200 SHEETS — FILLER

COMET